Separation Science and Technology
Publication details, including instructions for authors and subscription information:
http://www.informaworld.com/smpp/title~content=t713708471

SORPTION KINETICS FOR DYE REMOVAL FROM AQUEOUS SOLUTION USING ACTIVATED CLAY

Yuh-Shan Ho[a]; Chun-Chiao Chiang[b]; Yung-Chien Hsu[c]
[a] School of Public Health, Taipei Medical University, Taipei, Taiwan, Republic of China [b] Department of Chemical Engineering, Chin-Mim College, Taiwan, Republic of China [c] Department of Chemical Engineering, National Taiwan Institute of Technology, Taipei, Taiwan, Republic of China

To cite this Article Ho, Yuh-Shan , Chiang, Chun-Chiao and Hsu, Yung-Chien(2001) 'SORPTION KINETICS FOR DYE REMOVAL FROM AQUEOUS SOLUTION USING ACTIVATED CLAY', Separation Science and Technology, 36: 11, 2473 — 2488

To link to this Article: DOI: 10.1081/SS-100106104

URL: http://dx.doi.org/10.1081/SS-100106104

SEPARATION SCIENCE AND TECHNOLOGY, 36(11), 2473–2488 (2001)

SORPTION KINETICS FOR DYE REMOVAL FROM AQUEOUS SOLUTION USING ACTIVATED CLAY

Yuh-Shan Ho,[1],* Chun-Chiao Chiang,[2] and
Yung-Chien Hsu[3]

[1]School of Public Health, Taipei Medical University, No.
250, Wu-Hsing Street, Taipei, Taiwan, Republic of China
[2]Department of Chemical Engineering, Chin-Mim College,
No. 18, Shan Hu Li, Tou-Fen Town, Miao-Li, Taiwan,
Republic of China
[3]Department of Chemical Engineering, National Taiwan
Institute of Technology, No. 43, Keelong Road, Section 4,
Taipei, 106, Taiwan, Republic of China

ABSTRACT

The kinetics of Basic Red 18 and Acid Blue 9 sorption onto activated clay have been investigated. A batch sorption model, based on the assumption of a pseudo–second order mechanism, has been developed to predict the rate constant of sorption, the equilibrium sorption capacity, and initial sorption rate with the effect of initial dye concentration, activated clay particle size, temperature, and pH value. In addition, an activation energy of sorption has also been determined based on the pseudo–second order rate constants.

Key Words: Activated clay; Dye; Kinetics; Sorption

---

*Corresponding author. Fax: 886-2-2738 4831; E-mail: ysho@tmu.edu.tw

INTRODUCTION

A major interest in the use of cheap sorbents for the removal of dyes from aqueous effluents has been established during the past 20 years. Several sorbents have been successfully and economically used for dye removal, such as waste silica (1), hardwood sawdust (2), fly ash (3), chrome sludge (4), waste red mud (5), waste Fe(III)/Cr(III) hydroxide (6), waste banana pith (7), waste orange peel (8), biogas waste slurry (9), clay, bagasse pith, and maize cob, (10) and palm-fruit bunch (11). However, no kinetic model could be used for these sorption processes, probably because of the complicated sorption that is often categorized as two main types. The first type, physisorption, involves intermolecular forces, where the bonding between sorbent and sorbate is caused by Van der Waals forces and hydrogen bonds. The second type, chemisorption, involves valence forces in which electrons are covalently shared or exchanged between sorbent and sorbate.

The study of sorption kinetics in wastewater treatment is significant as it provides valuable insights into the reaction pathways and mechanisms of sorption reactions. Kinetics describe the solute uptake rate that controls the residence time of sorbate uptake at the solid-solution interface, and are important because to design appropriate sorption treatment plants, the rate at which any pollutant is removed from aqueous solutions must be predicted.

The pseudo–first order rate equation of Lagergren (12) has been widely applied since 1898. The earlier application of the pseudo–first order rate equation of Lagergren to the sorption of cellulose triacetate from chloroform on calcium silicate was undertaken by Trivedi, Patel, and Patel (13). Numerous studies report pseudo–first order Lagergren kinetics for the sorption of dyes, such as the sorption of Omega Chrome Red ME (a popular chrome dye) through a 1:1 ratio of fly ash to coal (14) and the sorption of methylene blue on water hyacinth roots (15). Table 1 shows a number of other pseudo–first order dye sorption systems.

In 1995, Ho (21) developed a pseudo–second order kinetic expression for the sorption system of divalent metal ions with sphagnum moss peat. It has also been applied to the sorption system of lead ions (22). The pseudo–second order rate equation of Ho has also been successfully applied to sorption systems such as those of basic and acid dyes with peat (23), wood (24), and pith (25).

The aim of this paper is to present an investigation of the kinetics of dye sorption when activated clay is used as the sorbent. The objective is to test the pseudo–second order model for analyzing the sorption of a basic dye, Basic Red 18 (BR18). and an acid dye, Acid Blue 9 (AB9), onto activated clay and to assess the usefulness and accuracy of the model. A study of the factors that affect the sorption kinetics includes the influence of the particle size of the activated clay, temperature, pH, and initial dye concentration. A rate parameter, k, has been defined and used to describe the sorption of acid dye onto activated clay.

Table 1. Pseudo–First Order Dye Sorption Systems Cited in Literature

Sorbent	Solute	Reference
Fly ash	Victoria Blue	(3)
Biogas residual slurry	Congo Red	(7)
Biogas residual slurry	Rhodamine-B	(16)
Biogas residual slurry	Acid Brilliant Blue	(17)
Biogas residual slurry	Direct Red 12 B	(18)
Fomitopsis Crania	Orlamar Red BG	(19)
Kaolinite	Bis Acid A2	(20)
Orange peel	Congo Red Procion Orange Rhodamine-B	(8)
Chrome sludge	Acid Blue 29 Reactive Blue 2	(4)
Red mud	Congo Red	(5)

EXPERIMENTAL

Materials

Sorbent

SiO_2 and Al_2O_3 are the major constituents of activated clay (Table 2), and other oxides are present in trace amounts. The activated clay was obtained from Laporte Industries (Singapore) Pte., Ltd.

Sorbate

The sorbates and their structures used in the experiments are listed below. The dyestuffs used consisted of commercial salts.

Testing solutions were prepared by placing separate dyestuffs BR18 and AB9 in reverse-osmosis treated water. The pH value was adjusted to 3.0 with HCl at 30°C. AB9 and BR18 solutions were filtered and then properly adjusted to appropriate concentrations for optical density measurements, and the calibration curves were established for each individual dyestuff.

Table 2. The Components of Activated Clay (% by Weight)

SiO_2	Al_2O_3	MgO	CaO	Fe_2O_3	$K_2O + Na_2O$	Ignition Loss
67–75	15–20	2.5	0.5	2.0	0.8	> 10

Basic Red 18 (C.I. Basic Red 18, C.I. 11085)

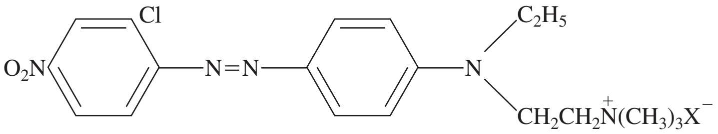

Acid Blue 9 (C.I. Acid Blue 9, C.I. 42090)

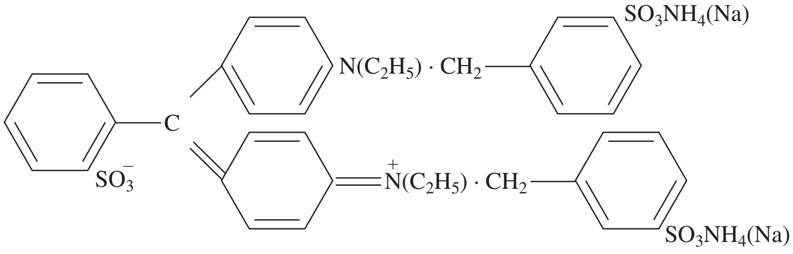

Methods

Dye solutions (500 mL) were prepared in reverse-osmosis treated water at pH 3.0 and maintained at a temperature of 30°C prior to the experiment (Solution A).

The activated clay particles were < 38 μm in diameter and had been dried in an oven (120°C) for more than 24 h. For all tests, the required amount of clay (2 g/dm^3 for BR18 and 3 g/dm^3 for AB9) was placed in a stirring chamber that contained 400 mL of reverse-osmosis treated water at pH 3.0 and maintained at a constant temperature of 30°C (Solution B).

Before mixing, 100 mL of Solution A was removed for the measurement of the initial dye concentration, while the remaining 400 mL was immediately decanted into Solution B for the adsorption experiment.

At intervals of 0.5, 1.0, 2.0, 5.0, 10.0, 30.0, 60.0, and 120.0 min, a 2 mL sample was withdrawn with a 20 mL syringe. It was then filtered through a membrane filter. The filtrate was diluted to a proper concentration for optical measurements.

The effect of experimental parameters, such as the initial dye concentration, the particle size of activated clay, the temperature, and initial pH value, were also studied (Tables 3–6). All experiments were carried out by changing one parameter at a time while holding the others constant.

Marcel Dekker, Inc.
270 Madison Avenue, New York, New York 10016

Table 3. Parameters for Particle Size Effect

	Basic Red 18				Acid Blue 9			
d_p	r^2	q_e	k	h	r^2	q_e	k	h
0–38	1.000	157	21.9	537	1.000	57.8	15.2	50.7
38–63	1.000	138	9.17	175	0.998	42.9	11.1	20.4
63–75	0.998	120	2.58	37.3	0.999	28.1	15.5	12.3
75–106	0.994	110	1.96	23.9	0.989	21.1	9.48	4.22

d_p (μm); q_e (mg/g); k ($\times 10^{-3}$ g/mg·min); h (mg/g·min).

Table 4. Parameters for Effect of Initial Concentrations

	Basic Red 18				Acid Blue 9		
C_0	r^2	q_e	k	C_0	r^2	q_e	K
111	1.000	54.3	174	59.7	1.000	7.29	99.3
213	1.000	105	11.9	114	1.000	13.8	43.9
326	1.000	157	2.19	356	1.000	41.1	4.41
367	1.000	165	2.81	475	1.000	53.4	2.12
443	1.000	185	1.50	552	1.000	58.2	1.49
520	1.000	208	1.69				

C_0 (mg/dm^3); q_e (mg/g); k ($\times 10^{-2}$ g/mg·min).

Table 5. AB9 Sorption Rate Dependence on Temperature

T (K)	r^2	q_e	k	h
283	1.000	82.2	1.19	80.3
293	1.000	65.9	1.29	55.9
303	1.000	61.1	1.34	49.9
313	1.000	56.4	1.45	46.1

q_e (mg/g); k ($\times 10^{-3}$ g/mg·min); h (mg/g·min).

Table 6. BR18 Sorption Rate Dependence on pH Value

pH	q_e	k	h	r^2
3.00	124	5.56	85.3	0.999
5.00	73.3	10.9	58.7	0.999
6.00	69.0	7.57	36.0	0.998
7.00	64.7	6.49	27.2	0.998
9.00	55.5	13.5	41.5	0.999
10.00	23.1	351	187	1.000

q_e (mg/g); k ($\times 10^{-3}$ g/mg·min); h (mg/g·min).

RESULTS AND DISCUSSION

Several steps can be used to express the mechanism of solute sorption onto a sorbent. To investigate the mechanism of sorption, the constants of sorption were determined by using a pseudo–second order mechanism.

The sorption kinetics may be described by the pseudo–second order model (21) that is shown in Eq. (1).

$$\frac{1}{(q_e - q_t)} = \frac{1}{q_e} + kt \tag{1}$$

Eq. (1) can be rearranged to a linear form:

$$\frac{t}{q_t} = \frac{1}{kq_e^2} + \frac{1}{q_e}t \tag{2}$$

and

$$h = kq_e^2 \tag{3}$$

The data in straight-line plots of t/q_t against t have also been tested to obtain rate parameters. The pseudo–second order rate constant, k, initial sorption rate, h, equilibrium sorption capacity, q_e, and correlation coefficients, r^2, for the dyes under variable conditions were calculated from the data represented in these plots.

Effect of Particle Size

Two series of experiments were carried out to study the influence of activated clay particle size. Figures 1 and 2 show the experimental results for the sorption of BR18 and AB9 onto activated clay. Table 3 shows that the sorption capacity of BR18 decreased from 157 to 110 mg/g as the activated clay particle sizes increased from 0–38 to 75–106 μm, while, the sorption capacity of AB9 decreased from 57.8 to 21.1 mg/g. This indicates that the smaller the activated clay particle size for a given mass of activated clay, the more surface area is available and as a consequence the greater the number of binding sites available. The kinetics of AB9 and BR18 sorption on activated clay follows the pseudo–second order rate expression. Linear plots of the t/q_t against t in Figs. 3 and 4 show the applicability of the pseudo–second order equation for the systems of BR18 and AB9 with activated clay particles ranging from 0–38 to 75–106 μm in diameter. The correlation coefficients, r^2, the pseudo–second order rate constants, k, the initial sorption rates, h, and the equilibrium sorption capacities, q_e, are presented in Table 3. The data show good compliance with the pseudo–second order equation because the regression coefficients are higher than 0.989 for all the systems in this study. The sorption process may involve a chemical reaction process and demon-

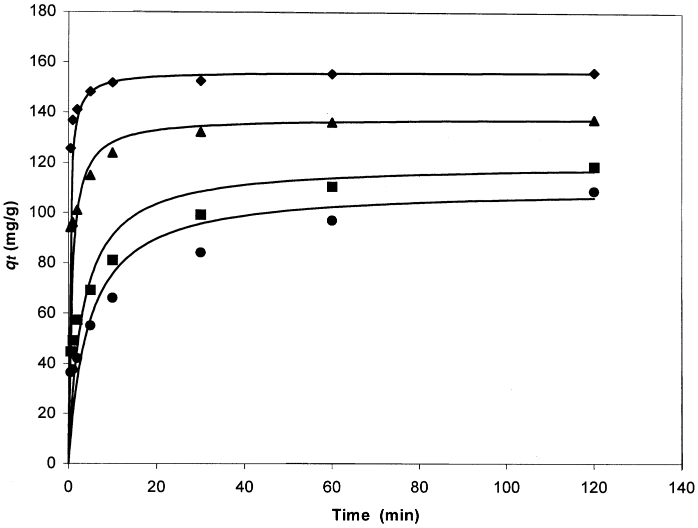

Figure 1. Plot of sorbed amount versus time for various sized particles of BR18: (◆) 0–38 μm, (▲) 38–63 μm, (■) 63–75 μm, (●) 75–106 μm, (—) second order model. Conditions: $C_0 = 300$ mg/dm^3; pH = 3.0; $T = 303$ K; $S = 500$ rpm; and $m_s = 2.0$ g/dm^3.

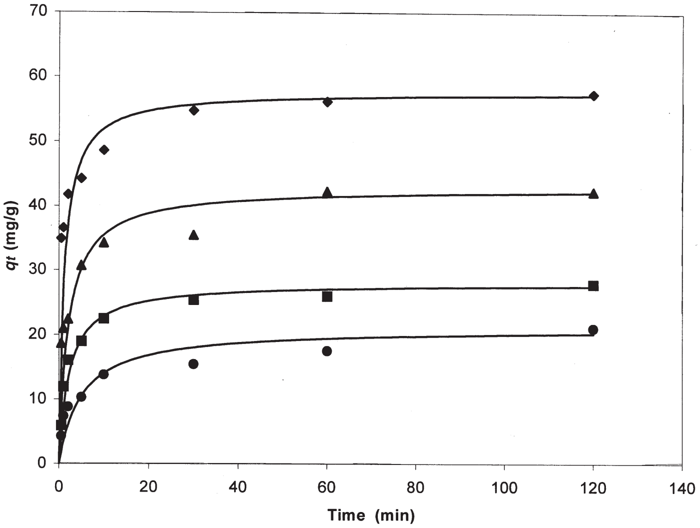

Figure 2. Plot of sorbed amount versus time for various sized particles of AB9: (◆) 0–38 μm, (▲) 38–63 μm, (■) 63–75 μm, (●) 75–106 μm, (—) second order model. Conditions: $C_0 = 300$ mg/dm^3; pH = 3.0; $T = 303$ K; $S = 500$ rpm; and $m_s = 3.0$ g/dm^3.

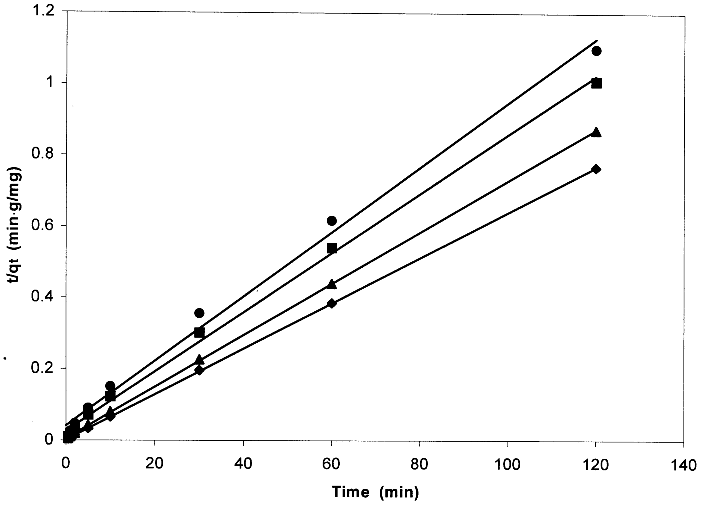

Figure 3. Pseudo–second order sorption kinetics of various sized particles of BR18 onto activated clay: (◆) 0–38 μm, (▲) 38–63 μm, (■) 63–75 μm, (●) 75–106 μm, (—) second order model. Conditions: C_0 = 300 mg/dm^3; pH = 3.0; T = 303 K; S = 500 rpm; and m_s = 2.0 g/dm^3.

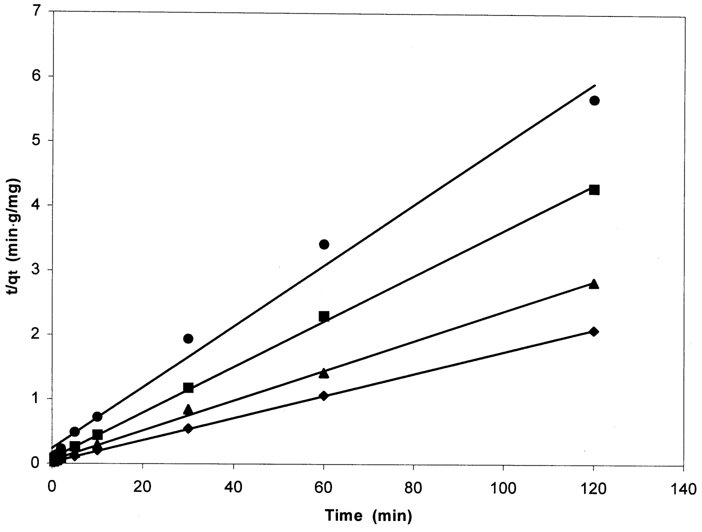

Figure 4. Pseudo–second order sorption kinetics of various sized particles of AB9 onto activated clay: (◆) 0–38 μm, (▲) 38–63 μm, (■) 63–75 μm, (●) 75–106 μm, (—) second order model. Conditions: C_0 = 300 mg/dm^3; pH = 3.0; T = 303 K; S = 500 rpm; and m_s = 3.0 g/dm^3.

strate that k is a function of the available surface area of the activated clay. The initial sorption rates also decreased with increased particle size. This would be expected because the amount of external surface area available for rapid reaction decreased with increased particle sizes for constant sorbent mass.

Effect of Initial Concentration

The influence of initial dye concentration was studied with BR18 and AB9. The kinetic data obtained from batch studies have been analyzed by using the pseudo–second order model developed by Ho (21) for the sorption of BR18 and AB9. The kinetics of BR18 and AB9 sorption on activated clay follows the pseudo–second order rate expression. Table 4 shows that the equilibrium sorption capacity increased from 54.3 to 208 mg/g as the initial concentration varied from 111 to 520 mg/dm^3 for BR18, and it increased from 7.29 to 58.2 mg/g as the initial concentration of AB9 increased from nearly 59.7 to 552 mg/dm^3. It is clear that the sorption capacity of basic dye is always much higher than acid dye in the activated clay sorption system. Similar results were observed by Ho and McKay for the sorption capacity of Basic Blue 69 and Acid Blue 25 onto peat (23) and onto wood (24); they found the same results for Basic Red 22 and Acid Red 114 onto pith (25). However, the values of the rate constant were found to decrease from 1.74×10^{-2} to 1.69×10^{-2} g/mg·min as the initial concentration increased from 111 to 520 mg/dm^3 for BR18, and it decreased from 99.3×10^{-2} to 1.49×10^{-2} g/mg·min as the initial concentration increased from nearly 59.7 to 552 mg/dm^3 for AB9. Ho and McKay presented similar results for the sorption systems of basic and acid dyes onto peat (23), wood (24), and pith (25). In addition, Table 4 shows good compliance with the pseudo–second order equation with the regression coefficients for the linear plots being higher than 0.999 for all the systems in this study.

Effect of Temperature

The temperature dependence of the sorption rates also is reflected in extremely high correlation coefficients. Figure 5 shows how temperature influences the time to reach saturation, and an excellent agreement exists between the experimental data and the theoretical curves that are predicted through the use of Eq. (1). The results suggest that the chemisorption reaction or an activation process was becoming more predominant in the rate-controlling step because Eq. (1) was based on the assumption of a chemical mechanism (21). Table 5 shows that the pseudo–second order rate constants for the AB9/activated clay system increased steadily with higher temperatures. The sorption capacity decreased from 82.2 to 56.4 mg/g and the initial sorption rate decreased from 80.3 to 46.1 mg/g·min

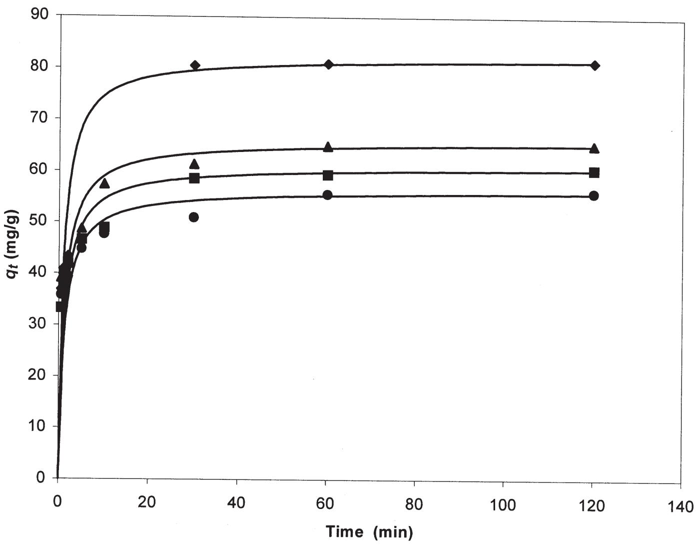

Figure 5. Plot of sorbed amount versus time for AB9 at various temperatures: (◆) $T = 283$ K; (▲) $T = 293$ K; (■) $T = 303$ K; (●) $T = 313$ K; (—) second order model. Conditions: $C_0 = 300$ mg/dm^3; pH = 3.0; $d_p = 0$–38 μm; $S = 500$ rpm; and $m_s = 3.0$ g/dm^3.

(Table 5), when the temperature increased from 283 to 313 K. The increase in the equilibrium sorption of AB9 with temperature indicates that a low temperature favors AB9 removal by sorption to activated clay because an elevation in temperature increases the escaping tendency of AB9 from an interface. This effect suggests that an explanation of the sorption mechanism associated with the removal of AB9 onto activated clay involves a physical process. A similar decrease in capacity was observed by Ho and McKay (23) with increasing temperature from 18 to 80°C in the case of the sorption of AB25 onto peat.

The values of k were found to increase from 1.19×10^{-2} to 1.45×10^{-2} g/mg·min, as the solution temperatures increased from 283 to 313K (Table 5). There is a linear relationship (Fig. 6) between the pseudo rate-constant and the reciprocal of the temperature: $r^2 = 0.983$. Therefore, the sorption rate constant may be expressed as a function of temperature by the following relationship:

$$k = k_0 \exp\left(\frac{-E}{RT}\right) \tag{4}$$

The relationship between k and T can be represented in an Arrhenius form as

$$k = 8.68 \times 10^{-2} \exp\left(\frac{-4.67 \times 10^3}{8.314T}\right)$$

In the equation, the temperature independent factor, k_0, is 8.68×10^{-2} g/mg·min. Furthermore, the activation energy of sorption, E, is 4.67 kJ/mole for the sorption system AB9 on activated clay. Because the sorption of AB9 onto activated clay is an exothermic process, an increasing solution temperature would be expected to result in a decreased sorption capacity.

Effect of Initial pH

Because ion exchange is one of the sorption processes, the rate of AB9 sorption onto activated clay was expected to vary by pH values of solution in the experiments. The pH values used in these studies were 3.00, 5.00, 6.00, 7.00, 9.00, and 10.00. Figure 7 shows that the sorption of AB9 was affected by the pH value and was represented linearly when AB9 uptake was plotted via the pseudo–second order equation (2). The values of k, q_e, and h of sorption at various pH values of BR18 are listed in Table 6.

The effect of pH on the sorption capacity of BH18 is shown in Fig. 8. The extent of sorption decreased from 124 to 23.1 mg/g when the pH of the system var-

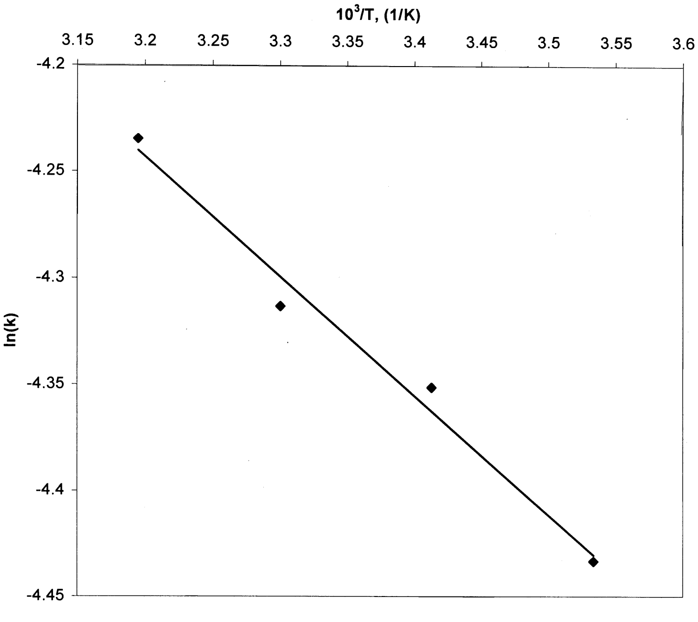

Figure 6. Plot of ln (k) against temperature for AB9 sorption onto activated clay. Conditions: $C_0 = 300$ mg/dm^3; pH = 3.0; $d_p = 0$–38 μm; $S = 500$ rpm; and $m_s = 3.0$ g/dm^3.

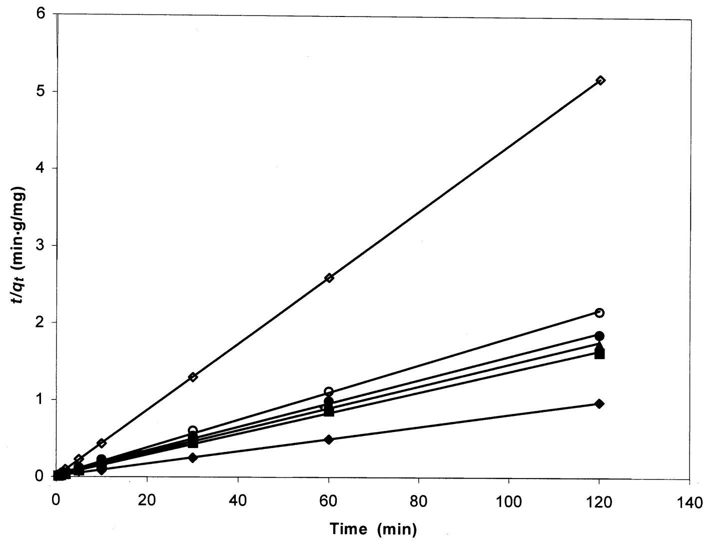

Figure 7. Pseudo–second order sorption kinetics of AB9 onto activated clay at various initial pH values. (◆) pH = 3; (■) pH = 5; (▲) pH = 6; (●) pH = 7; (○) pH = 9; (◇) pH = 10;(—) second order model. Conditions: $C_0 = 300$ mg/dm^3; $T = 303$ K; $d_p = 0$–38 μm; $S = 500$ rpm; and $m_s = 3.0$ g/dm^3.

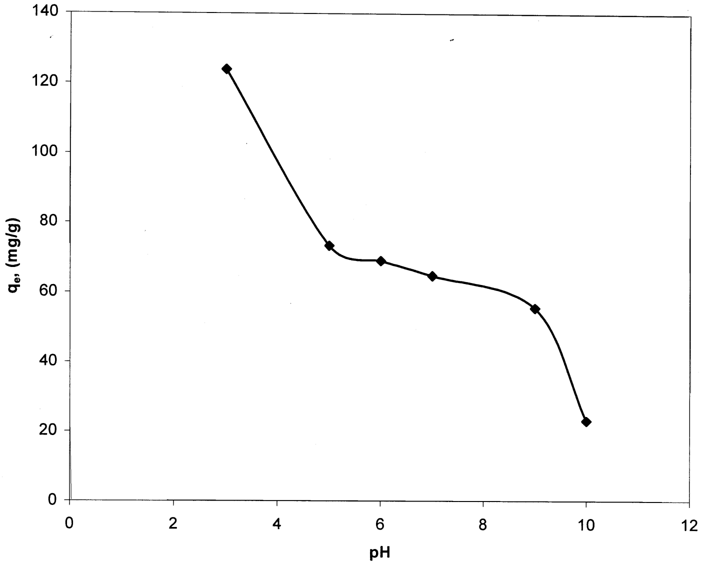

Figure 8. Plot of q_e against initial pH value for BR18 sorption onto activated clay. Conditions: $C_0 = 300$ mg/dm^3; $d_p = 0$–38 μm; $T = 303$ K; $S = 500$ rpm; and $m_s = 2.0$ g/dm^3.

ied from 3.00 to 10.00. The extent of dye removal decreased rapidly as pH increased from pH 3.00 to 5.00 and from 8.00 to 10.0. However, within the range of 5.00 to 8.00 it almost remained constant. The increase in sorption depends on the surface properties and dye structure. At a lower pH, the surface of the activated clay becomes negatively charged. At higher pH, it becomes positively charged. At a higher pH, the sorption of cationic dye should be less because of the higher dissociation of the dye molecules as well as the negatively charged surface. At a lower pH, both the dye and surface will be dissociated. This results in a lower sorption through decreased cation exchange capabilities. In addition, this effect may be explained on the basis of surface hydroxylation and acid-base dissociation and surface complexation (26). Similar descriptions have been reported for the sorption of acidic and basic dyes on kaolinite and montmorillonite (27), the sorption of dye on fly ash (28), the sorption of fluoride on fly ash (29), the sorption of basic dye on silica (30), the sorption of dye on china clay (31), and the sorption of color on chrome sludge (4).

CONCLUSIONS

The kinetics of sorption of BR18 and AB9 on activated clay have been studied on the basis of the pseudo–second order rate mechanism. The sorption capacity of basic dye (BR18) is much higher than acid dye (AB9) because of the ionic charges on the dyes and the character of the activated clay. The sorption capacity of dyes decreased as the activated clay particle sizes increased. A pseudo–second order model has been developed to predict the rate constant of sorption, the equilibrium sorption capacity, and the initial sorption rate. The use of these constants to generate the theoretically predicted curves shows that the kinetic model equation has an extremely high degree of correlation with the experimental data. The activation energy of sorption can be evaluated with pseudo–second order rate constants. The sorption of AB9 by activated clay is an exothermically activated process. The results show a good compliance with the pseudo–second order equation because the regression coefficients are high. The results suggest that the chemisorption reaction or an activation process were becoming more predominant in the rate-controlling step for both dye/activated clay systems.

NOMENCLATURE

C_0	concentration of dye in bulk liquid at $t = 0$ (mg/dm^3)
d_p	particle diameter (μm)
E	activation energy of sorption (kJ/mol)
h	initial sorption rate (mg/g·min)

k	equilibrium rate constant of pseudo–second order sorption (g/mg·min)
k_0	temperature independent factor (g/mg·min)
m_s	sorbent dose (g/dm^3)
q_e	amount of dye sorbed at equilibrium (mg/g)
q_t	amount of dye sorbed at specified time (mg/g)
R	gas constant (8.314 J/mol·K)
r^2	correlation coefficient
S	agitation speed (rpm)
T	solution temperature (K)
t	time (min)

REFERENCES

1. Alexander, F.; Poots, V.J.P.; McKay, G. Adsorpotion kinetics and diffusional mass transfer processes during color removal from effluent using silica. Ind. Eng. Chem. Process Des. Dev. **1978,** *17* (4), 406–410.
2. Asfour, H.M.; Fadali, O.A.; Nassar, M.M.; El-Geundi, M.S. Equilibrium studies on adsorption of basic dyes on hardwood. J. Chem. Technol. Biotechnol. **1985,** *35* (35A), 21–27.
3. Khare, S.K.; Panday, K.K.; Srivastava, R.M.; Singh, V.N. Removal of Victoria Blue from aqueous solution by fly ash. J. Chem. Technol. Biotechnol. **1987,** *38* (2), 99–104.
4. Lee, C.K.; Low, K.S.; Chow, S.W. Chrome sludge as an adsorbent for colour removal. Environ. Technol. **1996,** *17* (9), 1023–1028.
5. Namasivayam, C; Arasi, D.J.S.E. Removal of Congo Red from wastewater by adsorption onto waste red mud. Chemosphere **1997,** *34* (2), 401–417.
6. Namasivayam, C.; Thamaraiselvi, K.; Yamuna, R.T. Removal of paraquat by adsorption on ‘waste’ Fe(III)/Cr(III) hydroxide: Adsorption rates and equilibrium studies. Pestic. Sci. **1994,** *41* (1), 7–12.
7. Namasivayam, C.; Kanchana, N. Waste banana pith as adsorbent for color removal from wastewaters. Chemosphere **1992,** *25* (11), 1691–1705.
8. Namasivayam, C.; Muniasamy, N.; Gayatri, K.; Rani, M.; Ranganathan, K. Removal of dyes from aqueous solutions by cellulosic waste orange peel. Bioresource Technol. **1996,** *57* (1), 37–43.
9. Namasivayam, C.; Yamuna, R.T. Removal of Congo Red from aqueous solution by biogas waste slurry. J. Chem. Technol. Biotechnol. **1992,** *53* (2), 153–157.
10. Nassar, M.M.; El-Geundi, M.S. Comparative cost of color removal from textile effluents using natural adsorbents. J. Chem. Technol. Biotechnol. **1991,** *50* (2), 257–264.

Marcel Dekker, Inc.
270 Madison Avenue, New York, New York 10016

11. Nassar, M.M.; Hamoda, M.F.; Radwan, G.H. Adsorption equilibria of basic dyestuff onto palm-fruit bunch particles. Wat. Sci. Tech. **1995,** *32* (11), 27–32.
12. Lagergren, S. Zur theorie der sogennanten adsorption gelöster stoffe. K. Sven. Vetenskapsakad. Handl. **1898,** *24* (4), 1–39.
13. Trivedi, H.C.; Patel, V.M.; Patel, R.D. Adsorption of cellulose triacetate on Calcium silicate. Eur. Polym. J. **1973,** *9,* 525–531.
14. Gupta, G.S.; Prasad, G.; Singh, V.N. Removal of chrome dye from aqueous solutions by mixed adsorbents: Fly ash and coal. Water Res. **1990,** *24* (1), 45–50.
15. Low, K.S.; Lee, C.K.; Tan, K.K. Biosorption of basic dyes by water hyacinth roots. Bioresource Technol. **1995,** *52* (1), 79–83.
16. Namasivayam, C.; Yamuna, R.T. Removal of Rhodamine-B by biogas waste slurry from aqueous solution. Wat. Air Soil Pollut. **1992,** *65* (1–2), 101–109.
17. Yamuna, R.T.; Namasivayam, C. Color removal from aqueous solution by biogas residual slurry. Toxicol. Environ. Chem. **1993,** *38* (3–4), 131–143.
18. Namasivayam, C.; Yamuna, R.T. Adsorption of Direct red 12 B by biogas residual slurry. Environ. Pollut. **1995,** *89* (1), 1–7.
19. Mittal, A.K.; Gupta, S.K. Biosorption of cationic dyes by dead macro fungus *Fomitopsis carnes*: Batch studies. Wat. Sci. Tech. **1996,** *34* (10), 81–87.
20. Atun, G.; Sismanoglu, T. Adsorpotion of 4,4'dioxyaceticacid from aqueous solution on kaolinite. J. Environ. Sci. Health Part A Environ. Sci. Eng. **1996,** *31* (8), 2055–2069.
21. Ho, Y.S. Adsorption of heavy metals from waste streams by peat. Ph.D. Thesis, The University of Birmingham, U.K., 1995.
22. Ho, Y.S.; McKay, G. Kinetic model for lead (II) sorption on to peat. Adsorption Sci. Technol. **1998,** *16* (4), 243–255.
23. Ho, Y.S.; McKay, G. Sorption of dye from aqueous solution by peat. Chem. Eng. J. **1998,** *70* (2), 115–124.
24. Ho, Y.S.; McKay, G. Kinetic models for the sorption of dye from aqueous solution by wood. Proces Saf. Environ. Protect. **1998,** *76* (B2), 183–191.
25. Ho, Y.S.; McKay, G. A kinetic study of dye sorption by biosorbent waste product pith. Resour. Conserv. Recy. **1999,** *25* (3–4), 171–193.
26. Ahmed, S.M. Studies of the dissociation of oxide surfaces at the liquid-solid interface. Can. J. Chem.—Rev. Can. Chim. **1966,** *44,* 1663–1670.
27. Sethuraman, V.V.; Rayamahashay, B.C. Color removal by clays: Kinetic study of adsorption of cationic and anionic dyes. Environ. Sci. Technol. **1975,** *9* (13), 1139–1140.
28. Gupta, G.S.; Prasad, G.; Panday, K.K.; Singh, V.N. Removal of chrome dye from dye aqueous solutions by fly ash. Wat. Air Soil Pollut. **1988,** *37* (1–2), 13–24.

29. Chaturvedi, A.K.; Yadava, K.; Pathak, K.C.; Singh, V.N. Defluoridation of water by adsorption on fly ash. Wat. Air Soil Pollut. **1990,** *49* (1–2), 51–61.
30. Ahmed, M.N.; Ram, R.N. Removal of basic dye from waste-water using silica gel as adsorbent. Environ. Pollut. **1992,** *77* (1), 79–86.
31. Gupta, G.S.; Shukla, S.P.; Prasad, G.; Singh, V.N. China clay as an adsorbent for dye house wastewaters. Environ. Technol. **1992,** *13* (10), 925–936.

Received August 1999
Revised March 2000

Marcel Dekker, Inc.
270 Madison Avenue, New York, New York 10016

Downloaded At: 10:44 25 January 2011

Request Permission or Order Reprints Instantly!

Interested in copying and sharing this article? In most cases, U.S. Copyright Law requires that you get permission from the article's rightsholder before using copyrighted content.

All information and materials found in this article, including but not limited to text, trademarks, patents, logos, graphics and images (the "Materials"), are the copyrighted works and other forms of intellectual property of Marcel Dekker, Inc., or its licensors. All rights not expressly granted are reserved.

Get permission to lawfully reproduce and distribute the Materials or order reprints quickly and painlessly. Simply click on the "Request Permission/Reprints Here" link below and follow the instructions. Visit the U.S. Copyright Office for information on Fair Use limitations of U.S. copyright law. Please refer to The Association of American Publishers' (AAP) website for guidelines on Fair Use in the Classroom.

The Materials are for your personal use only and cannot be reformatted, reposted, resold or distributed by electronic means or otherwise without permission from Marcel Dekker, Inc. Marcel Dekker, Inc. grants you the limited right to display the Materials only on your personal computer or personal wireless device, and to copy and download single copies of such Materials provided that any copyright, trademark or other notice appearing on such Materials is also retained by, displayed, copied or downloaded as part of the Materials and is not removed or obscured, and provided you do not edit, modify, alter or enhance the Materials. Please refer to our Website User Agreement for more details.

Order now!

Reprints of this article can also be ordered at

http://www.dekker.com/servlet/product/DOI/101081SS100106104